Redistribution of resonance radiation in hot and dense plasmas

C. Mossé, A. Calisti, R. Stamm, and B. Talin
UMR 6633–case 232, Université de Provence, Centre St. Jérôme, 13397 Marseille Cedex 20, France

R. Lee
Lawrence Livermore National Laboratory, P.O. Box 808, L-399 Livermore, California 94550

L. Klein
Department of Physics, Howard University, Washington, D.C. 20059
(Received 19 January 1999)

A method for calculating the redistribution of resonance radiation in hot, dense plasmas is developed by extending the frequency fluctuation model (FFM). This model was originally designed as a numerical procedure for the calculation of the spectral shape of Stark-broadened lines emitted by multielectron ions and has been particularly useful in computations accounting for the ion dynamics effect. The FFM is based on a numerical technique that replaces the primitive inhomogeneous Stark component contributions to the linear response line shape with the observable radiative channels. These channels can be viewed as equivalent to a system of microfield dressed two-level radiators, the Stark-dressed transitions (SDT), which emit a set of spectral lines that reproduce the main features of the first-order radiative properties of the emitter. The mixing of these transitions through a stochastic process is equivalent to random fluctuations of the local ion microfield. The SDT form the basis for the extension of the FFM to the computation of nonlinear response functions. The theory of the second-order radiative redistribution function is reviewed and examples are given.
[S1050-2947(99)08008-7]

PACS number(s): 32.70.−n, 52.25.Qt, 95.30.Jx

I. INTRODUCTION

Recent advances in the computation of the radiative properties of complex ions in hot, dense plasmas, made possible by the development of the frequency fluctuation model (FFM) [1], have resulted in an adequate understanding of the effect of the plasma environment on the emission or absorption process and the shape of the associated spectral lines [2]. In addition, the FFM treatment of ion-field fluctuations has resulted in line-shape calculations that provide good diagnostics of the plasma parameters under a wide range of conditions [3–5]. The next logical step in understanding the radiative properties of hot, dense plasmas is to develop models for the study of the multiphoton response, e.g., the scattering of resonance radiation. One motivation for this study is that for lines with a large optical depth there remain difficult problems involving radiative transfer. Beyond the simplest assumption that the line shape is independent of the radiative redistribution, these problems cannot be understood simply through calculations of the one-photon absorption or emission spectrum, but require the development of a computational ability to treat the scattering of near-resonant radiation in hot, dense plasmas. This means that a theoretical formulation of the two-photon plasma spectral properties in the presence of a combination of homogeneous and inhomogeneous broadening processes must be developed. In the following, this will be accomplished by extending the usual linear response formulation of the spectral line shape to the higher-order absorption and re-emission response function that is required for the computation of radiation redistribution.

Two basic radiative redistribution processes can be considered. The first is the straightforward observation of the scattered photons from a plasma subjected to a radiation source. A possible experimental observation of this type is the pumping of the ground state of a transition with a source created from the excited state of the same transition. This is the technique utilized in the first observations of photopumping in high-Z plasmas in which a hot, laser-produced aluminum plasma-produced lines from He-like ions that were used to pump ground-state He-like ions in another, spatially distinct, but more dense, aluminum plasma [6]. Another example of this process is the familiar monochromatic pump-fluorescence experiment. To significantly scatter the pumping radiation in experiments of this type, the target plasma must be prepared so that the optical depth is small for the considered transition, e.g., the lower level of the transition is well populated. Recent progress has resulted in the development of x-ray lasers with wavelengths appropriate for photopumping ground-state transitions of multielectron ions [7] that have sufficient brightness to make them suitable for use as resonant photoexcitation sources [8] in experiments of this type. Since these x-ray lasers are not tunable, only ionic transitions that have a near resonance with specific laser wavelengths can be studied. Using tables of transition wavelengths [9], one of the $3d$-$2p$ lines of fluorinelike magnesium, which at 146.526 Å is separated by only 11 mÅ from the zirconium 146.515-Å x-ray laser line, was identified as a possible candidate for an experiment, and a preliminary study on the feasibility of this case has been published [10].

The second basic process involving radiative redistribution involves cases related to radiative transfer. The observation of the modification of the spectrum of radiation propa-

gating in a plasma with large optical depth is an example of this type of process. This case requires a more general theoretical discussion of the effect of redistribution on radiation transport in plasmas near ionic resonances. In addition to the plasma conditions, this process strongly depends on the geometry of the experiment. Thus, we cannot formulate a general calculation of a typical experiment as was done for the study of the feasibility of direct redistribution [10]. In general, considerations of radiation transport give rise to complex problems involving both nonlinear mechanisms and resonant diffusion in addition to inhomogeneous line broadening. An example involving the Balmer alpha transition of hydrogenlike carbon has been discussed in the context of x-ray laser gain studies [11]. The results presented later in Sec. V for this transition will be limited to an examination of the redistribution function for hydrogenlike carbon plasma conditions and will not address the more complicated radiative transfer issues.

Section II of this paper is devoted to a brief review of line-shape theory in the linear-response approximation, and an introduction to the FFM approach to the modeling of line shapes in plasmas. This discussion begins with a consideration of the spectral lines emitted by complex ions in plasmas. As is well known, the line shape is determined by the time-dependent coupling of the ion with the plasma environment. This plasma-emitter interaction leads to Stark broadening of the spectral lines, and traditionally has been considered in the approximation that treats the effect of the electrons on the emitting ion in the impact limit while the ionic perturbation is taken to be quasistatic. In this approximation, the time dependence of the perturbation has been eliminated, resulting in a spectral line shape that has purely homogeneous and inhomogeneous contributions and that is described by a simple sum of independent electron-impact-broadened static components.

Although the electron collisions are often well described by the impact approximation, it is well known that a quasistatic treatment of the ion perturbation can lead to large errors for plasma conditions that yield substantial ion-field fluctuations [12]. In Sec. II, to incorporate these time-dependent ion perturbation effects into a calculation of the spectrum, the FFM model is introduced [13]. As a first step, the impact electron, quasistatic ion approximation that results in the profile described by an independent sum of static Stark components, is taken as a zero-order approximation, perturbed by the time dependence of the ion interaction. In this formulation the fluctuating ion interaction modifies the inhomogeneous ion broadening, by replacing the quasistatic ion field interaction by a fluctuating perturbation acting on the homogeneous electron-impact-broadened resonances. In first approximation, this results in an enlarged homogeneous broadening and a residual inhomogeneous contribution due to a subset of the ions. The associated modification of the line shape is usually referred to as the ion dynamics effect.

Before modifying the ion perturbation to include the ion dynamics effect, however, since the individual Stark components are not separately observable, we replace them by a reduced set of observable resonances, the Stark-dressed transitions (SDT), or equivalently, dressed two-level systems. In this description, the set of independent static Stark components that compose the transition in the static ion approximation is replaced by a set of independent SDT that form the same overall spectral profile. This permits a simple interpretation of the fluctuation of the inhomogeneous components in the ion dynamics effect as being a mixing of the SDT through a stochastic exchange mechanism [13]. Assuming a Markovian exchange process between the SDT, the mixing process can cause them to overlap and merge. Comparisons with computer experiments based on a full simulation of the plasma indicate that the FFM accurately describes the ion dynamics effect [2] for a wide range of plasma conditions. The use of this ion microfield-dressed emitter model permits the memory of the original (static) inhomogeneous spectral characteristics of the line shape to be retained throughout the subsequent dynamic calculation.

The modification of the FFM for the computation of the redistribution function is presented in Sec. IV where the one-photon spectral line formalism of the FFM is extended to include two-photon processes. The ion microfield-dressed emitter representation is used to evaluate the second-order pump-fluorescence radiative response to obtain a description of the frequency dependence of the fluorescence emitted by an ion that has absorbed a photon near spectral resonance. Because the spectral shape of the fluorescence depends strongly on the mixing rate induced by the plasma, the ion dynamics effect must be included. Therefore, a static model with the associated set of two-level transitions without exchange, cannot fully describe the response to monochromatic pumping.

In order to clarify the concepts presented, examples of radiative redistribution functions for simple cases are presented in Sec. V. Included is an example of an x-ray laser-pumped system that illustrates the capability of the model to provide a sensitive method for the study of radiative transfer under plasma conditions of partial redistribution. That is, in cases where the strong mixing limit is not attained so that the mixing of the inhomogeneous spectral line components is not fast enough to produce a completely redistributed line. The complete redistribution limit is the most common assumption in redistribution studies and is equivalent to postulating that the scattered radiation has the same spectral shape as the absorption line. More generally, partial redistribution results in a fluorescence spectra consisting of a sharp coherent Rayleigh peak centered on the frequency of the incident radiation and a redistribution line emitted near the resonance frequency. This pattern of coherently scattered and redistributed radiation has been observed under a variety of experimental conditions for neutral emitters in gases [14] or plasmas [15,16]. However, until recently, x-ray spectroscopy in hot and dense plasmas could not be applied to redistribution measurements with the same precision as in the neutral gas domain. X-ray laser pumping could change this situation, and provide data of sufficient quality that accurate calculations of radiative transfer in dense plasmas could be tested.

II. LINEAR RESPONSE: THE ONE-PHOTON SPECTRAL LINE SHAPE

The expression for the linear response of a plasma-emitter system to an unpolarized monochromatic electromagnetic wave of angular frequency ω is determined by the response function $G(\omega)$, which is the one-sided Fourier transform of

the bath-averaged evolution operator of the emitter $U(t)$,

$$G(\omega)=\frac{-i}{\pi}\int_0^\infty e^{i\omega t}U(t)dt=(\omega-L_0)^{-1}, \tag{1}$$

where L_0 is the Liouville operator for the system evolution alone. The line-shape function in the radiative dipole approximation is related to the imaginary part of the Fourier-transformed dipole autocorrelation function. This can be written as a normalized Liouville space-matrix element of the response function,

$$I(\omega)=\mathrm{Im}\langle\langle d^\dagger|G(\omega)|d\rho_0\rangle\rangle, \tag{2}$$

where ρ_0 is the equilibrium density-matrix operator for the active quantum system, and d is the dipole operator for the emitting quantum system. In Liouville space notation, $\langle\langle d^\dagger|d\rangle\rangle=\mathrm{Tr}\{d^\dagger d\}$, where the trace is taken over the sublevels of the two states involved in the radiative transition under consideration. The subsequent calculation of the pump-fluorescence spectrum will require higher, nonlinear response terms that have a simple relation to this function. An average over the polarization is understood in the above since unpolarized radiation has been assumed. Polarization effects associated with the redistributed radiation will be ignored for simplicity in the following, limiting the subsequent development to one-dimensional scattering.

To account for ion dynamics, the microfield interaction must be treated as time-dependent. This means that if we consider the interaction fluctuations or collisions to be random, a stochastic Liouville equation must be solved to obtain $G(\omega)$. However, in the FFM, instead of attempting an exact solution of the complete equation for $G(\omega)$, the line-shape calculation is initially performed by treating the electron collisions as impacts and the ion perturbation as quasistatic. The time dependence is introduced at a later stage of the calculation. The result of this initial assumption is that the quantum-emitter system evolution operator in Eq. (2), contains in the Liouville operator a non-Hermitian, homogeneous electron-impact broadening contribution, which is numerically averaged over the ion microfield interaction with a stationary-field probability distribution. For each radiative transition, this procedure yields a spectral line-shape function that can be written as a sum of rational fractions or generalized Lorentzian spectral components of the line [2]. These are the static Stark components, each of which is characterized by a complex frequency and intensity. They are complex, because of the non-Hermitian collision operator, used to describe the impact electrons.

The Stark components are the basic data for the FFM, but are not necessarily distinct or observable quantities. To reduce the computation to a more manageable size, appropriate for the later introduction of time dependence in the Stark interaction, we introduce the radiative channels, a set of objects having more physical meaning. These are defined as the smallest observable resonant features that can be extracted from the quasistatic profile. As defined, an FFM radiative channel also can be considered as equivalent to a two-level transition dressed by the quasistatic ion microfield interaction, the SDT. The SDT substitution is accomplished through a numerical coarse-graining analysis in the frequency-linewidth space of the Stark component set and is equivalent to a numerical merging procedure that combines the Stark components that are within a prescribed neighborhood. This procedure preserves the inhomogeneous structure of each Stark-broadened radiative transition as well as that due to the various radiative transitions that are in the spectral domain of interest. The SDT are the fundamental observable components of the quasistatic line shape. Like the primitive Stark components, each SDT is characterized by two complex numbers. These are the generalized frequency, $f_i-i\gamma_i$, and the generalized intensity, a_i+ic_i. The linear response line-shape function for a given transition with n SDT can be written in this approximation as a sum over the SDT,

$$I(\omega)=\sum_{i=1}^{n}\frac{c_i(\omega-f_i)+a_i\gamma_i}{(\omega-f_i)^2+\gamma_i^2}. \tag{3}$$

It has been shown by direct comparison that the change in $I(\omega)$ is insignificant when these distinct radiative channels are introduced to replace the primitive Stark components.

III. FREQUENCY FLUCTUATION MODEL

The FFM is based on the premise that a quantum system perturbed by an electric microfield behaves like a set of dressed two-level transitions, the SDT. If the ion microfield is time varying, then the set of transitions are subject to a collision-type mixing process induced by the field fluctuations. To proceed, the Liouville space of these two-level dressed emitters is extended to include the SDT index so that the basis set of eigenvectors in this space, $\{|eg;i\rangle\rangle\}$, are now labeled by the quantum states of the emitters (e,g) and, in addition, by the channel number. In this space, we can rewrite the linear response line-shape function of Eq. (3) in terms of dressed two-level radiators by defining a generalized dipole moment matrix element $(\mathbf{D}_i)_{eg}$ for the SDT. This can be done by relating the amplitude of the SDT dipole moment matrix element to the intensity of the transition associated with the coupling of the radiation field to the upper and lower levels, e and g, of the ith dressed two-level system or SDT. The normalized matrix element is

$$(\mathbf{D}_i)_{eg}=r\sqrt{(1+ic_i/a_i)}, \tag{4}$$

where $r=\sqrt{\Sigma a_k}$ is the reduced matrix element of the transition associated with the emission of the SDT. This generalized dipole moment matrix element can be considered to be the diagonal element of the ith component of a vector operator $\mathbf{D}$, which acts in the extended Liouville space. We also define the probability vector operator $\mathbf{p}$ with element $(p_i)_{eg}$ describing the instantaneous probability of occurrence of a particular radiative channel (the ith SDT with upper and lower states, e and g). This probability is determined by the normalized real part of the amplitude or relative intensity of the channel

$$p_i=a_i/r^2. \tag{5}$$

The linear response line shape of Eq. (3), in the quasistatic ion, impact-electron approximation can now be normalized and written as an average over the initial and sum over the final SDT in the extended Liouville space as

$$I(\omega)=\mathrm{Im}\sum_{i,f}\ p_i(\langle\langle\mathbf{D}|\mathbf{G}^0(\omega)|\mathbf{D}\rho_0\rangle\rangle)_{i,f}, \tag{6}$$

where

$$\mathbf{G}^0(\omega)=(\omega\mathbf{1}-\mathbf{L}_0)^{-1}, \tag{7}$$

and **1** is the unit operator. It is noted that the initial and final states may include states of different principal quantum numbers as required to obtain a correct description of the line profile [17]. The Liouville operator $\mathbf{L}_0$ has a set of eigenfrequencies, $\omega_i=f_i-i\gamma_i$, composed of the generalized frequencies and widths of the SDT. The Liouville space matrix element of the propagator in Eq. (6) is a trace over the SDT states, which include the emitter-plasma interaction. The ion microfield is considered to be quasistatic at this point, so that, in this approximation, the propagator $\mathbf{G}^0(\omega)$ is diagonal in the SDT index and the FFM line shape is a sum of independent contributions from a set of generalized Lorentzian terms, or radiative channels. Each independent term in this sum is to be associated with the emission from one of the n SDT that interact with the radiation field through the generalized dipole moment **D** of Eq. (4). The next step is to extend this formulation to include ion dynamics, i.e., the time-dependent effect of a fluctuating ion microfield on the spectral line shape.

The ion dynamics is included in the FFM through the hypothesis that the time dependence of the fluctuating ion microfield causes a mixing of the SDT. When only one Stark-broadened radiative transition is considered at a time, the slowly varying ion Stark effect is assumed to transfer population between different radiative channels. This transfer is observed in the absorption or emission spectrum as an exchange mechanism, which mixes the formerly separate SDT. The degree of deviation from a sum of independent Lorentzian lines (the quasistatic spectrum) is a measure of the ion microfield fluctuation rate. In the next section, the mixing rate of the various level populations will be seen to be an observable in the redistribution spectrum. This is not the case with an absorption or emission spectrum that depends only on the transition amplitudes. In order to guarantee the appropriate limits for slow and fast field fluctuation, only SDT that originate from the same radiative transition are included in the mixing processes considered in the following. However, to model more general cases than those considered here, like those with fine-structure levels perturbed by inelastic collisions, an exchange process between radiative transitions should be taken into account.

The exchange mechanism mixing the SDT and associated levels is assumed to be a Markov process. Such a process is completely determined by two sets of quantities: the instantaneous SDT probability operator **p**, with elements defined in Eq. (5), and a transition rate operator **W**. The elements of **W** are of two types: those that correspond to dressed level mixing rates $(\mathbf{W})_{kk}$ and those that refer to dressed transition (or coherence) mixing rates $(\mathbf{W})_{kl}$. For the linear absorption or emission spectra considered in this section, the propagator in Eq. (6) is to be calculated in the transition subspace, $\{|eg;i\rangle\rangle\}$, where e is the excited and g is the lower state of the SDT. Therefore, the only parameters required for the spectrum of a given radiative transition are the elements of **p**, $(p_i)_{eg}$, and the elements of the coherence mixing rate matrices $(\mathbf{W})_{eg}$ or $(\mathbf{W})_{eg}$.

The mixing rate elements represent ion motion effects, and can be parametrized by the characteristic microfield fluctuation frequency ν so that the Markov mixing process is determined uniquely by the probability p_i and fluctuation frequency ν. For weakly coupled plasmas, the random ion motion, in general, dominates the collective motion and the characteristic fluctuation frequency is no longer the plasma frequency ω_p but depends on the ionic thermal velocity $\langle v\rangle$ and the average ionic separation r_0. Because of the long range of the Coulomb interaction, even if screened, the microfield at the emitter can be considered to be due to a particular configuration of a number of ions. To obtain an expression for the characteristic frequency we assume, using dimensional arguments that this frequency will be related to $\nu=K\langle v\rangle/r_0$, where K may be evaluated by determination of the ion microfield fluctuation rate. In the present case we assume the simplistic model that $K=1$ in keeping with the nature of the present results.

The transition rate operator **W** is diagonal in the radiative channel level indices eg but not in the channel index i. It has diagonal and off-diagonal elements, $(W_{i,i})_{eg}$, and $(W_{i,j})_{eg}$ that are, respectively, the inverse lifetime and the rate of mixing of the radiative channel transitions. To insure detailed balance in the model, the probability and rate elements must be connected,

$$(W_{ij})_{eg}=-\nu(p_i)_{eg}\quad(i\neq j),\quad (W_{ii})_{eg}=\nu[1-(p_i)_{eg}]. \tag{8}$$

The linear-response line shape resulting from the stochastic mixing of the radiation channels can be written in the Liouville space of the dressed two-level radiators in the same form as Eq. (6), but with $\mathbf{G}^0(\omega)$ replaced by

$$\tilde{\mathbf{G}}^0_W(\omega)=(\omega\mathbf{1}-\mathbf{L}_0+i\mathbf{W})^{-1}. \tag{9}$$

The diagonal operator $\mathbf{L}_0$ is that of Eq. (7) with the same SDT eigenfrequencies, $\omega_i=f_i-i\gamma_i$. Since the dressed two-level systems are coupled together by the exchange operator **W** the FFM line shape is no longer a simple sum of n-independent SDT lines. In addition, this model has appropriate fluctuation frequency rate limits for the dynamics of the ion microfield. The quasistatic limit is obtained for a vanishing fluctuation rate and the field-free case is recovered in the infinite fluctuation rate limit. As mentioned in the Introduction, calculations of the spectral line shape of ion emitters in hot, dense plasmas have been performed with the FFM and comparisons with experiments have verified the accuracy of the theory [3–5].

IV. REDISTRIBUTION

The one-photon emission or absorption spectroscopy model described above is extended now to two-photon redistribution by continuing the expansion of the response function to higher order in the emitter-radiation field interaction [18]. This is performed by obtaining an iterative solution to the equation for the density operator to replace the equilibrium solution used in Eq. (2). The higher-order radiative re-

sponse functions that arise describe either redistribution, where the power spectrum of the fluorescence induced by monochromatic pumping radiation is studied [10,19], or pump-probe phenomena where the change of the linear radiative response due to a pump field is considered [20]. In this paper only redistribution will be considered. This approach is based on a previous investigation of the fluorescence of simple two- or three-level atomic systems in a plasma [21]. Here we treat complex multielectron ion emitters and hot and dense plasma conditions. The SDT picture permits a simple extension of the FFM to the calculation of these higher-order response functions. Since the emitter-plasma interaction is incorporated in the SDT, the only interaction term in the Liouville propagator for the plasma-dressed emitter propagator of Eq. (9) is the Markov channel mixing process $\mathbf{W}$. By definition, all other interaction terms have been incorporated into the SDT.

To calculate the spectrum of radiation scattered by an ionic emitter in a plasma, the monochromatic laser field will be assumed to have a frequency near one of the ion resonances. The interaction is described by the operator, $\mathbf{V}_S$ or $\mathbf{V}_L$, the field interaction operators for the coupling of the spontaneous emission or the incoming pump radiation, respectively, with the generalized dipole operator of the SDT. The field interaction operators are time-dependent and have the form

$$\mathbf{V}_R(t)=\mathbf{V}_R^+ e^{-i\omega_R t}+\mathbf{V}_R^- e^{i\omega_R t}, \tag{10}$$

where $\mathbf{V}_R^{\pm}=\mathbf{D}\cdot\mathbf{E}_R^{\pm}$ is the SDT-radiation field dipole interaction. The field amplitude $\mathbf{E}_R$ and frequency $\omega_R=ck_R$ refer to the pump field for $R=L$ and the spontaneous emission field for $R=S$.

The power spectrum of the radiation emitted at frequency ω_S by a system pumped at frequency ω_L can be written [18]:

$$I(\omega_S,\omega_L)\propto \lim_{\eta\to 0}\ \mathrm{Im}\sum_{i,f}\ p_i(\langle\langle \mathbf{V}_S|\mathbf{G}_W(i\eta)|\mathbf{V}_L\rho_0\rangle\rangle)_{i,f}, \tag{11}$$

where $\mathbf{G}_W(i\eta)$, the Fourier transform of the evolution operator for the SDT, now contains in addition, the radiation field dipole interaction in the Liouville operator. As in Eq. (6), the SDT picture has been used to replace the average over the ion microfield states by an average over the initial SDT states with probability p_i and a sum over the final states.

To remove the explicit time dependence in Eq. (11), the Liouville space basis is augmented to include Floquet numbers n_L that count the number of harmonics of the pump frequency ω_L present in each order of the response calculation. It is also generalized to include the photon numbers, n_e and n_g, for the spontaneous emission or absorption at the frequency ω_S by the corresponding SDT [22]. The eigenstates in this space are now denoted $|eg,i,n_L,n_e,n_g\rangle\rangle$. The Floquet-photon number operator Ω is diagonal in this basis set with eigenvalues denoted $[n_L\omega_L+(n_e-n_g)\omega_S]$.

The $\eta\to 0$ limit of the propagator in Eq. (11) is written as an operator in this extended space as

$$\mathbf{G}_W(\Omega)=[\Omega-\mathbf{L}_0+i\mathbf{W}-(\mathbf{V}_S+\mathbf{V}_L)]^{-1}, \tag{12}$$

and satisfies the Dyson equation

$$\mathbf{G}_W(\Omega)=\mathbf{G}_W^0(\Omega)+\mathbf{G}_W^0(\Omega)(\mathbf{V}_S+\mathbf{V}_L)\mathbf{G}_W(\Omega), \tag{13}$$

where $\mathbf{G}_W^0(\Omega)=(\Omega-\mathbf{L}_0+i\mathbf{W})^{-1}$ is the analog of the field-free operator of Eq. (9) defined in the extended Liouville-Floquet space. In the following, we shall consider only those experiments that involve monochromatic pumping intensities with Rabi frequency small compared to the relaxation parameters of the emitter. Then, the pump field is sufficiently weak that the iteration of the Dyson equation (13) can be terminated at the lowest nonvanishing order. The Floquet-photon number matrix element of the propagator of Eq. (11) becomes in this approximation,

$$\begin{aligned} I(\omega_S,\omega_L)\propto \mathrm{Im}\sum_{i,f}\ p_i(\langle\langle \mathbf{V}_S|\mathbf{G}_W^0(\omega_S)&\\ \times\{\mathbf{V}_L\mathbf{G}_W^0(\omega_S-\omega_L)\mathbf{V}_S\mathbf{G}_W^0(-\omega_L)&\\ +\mathbf{V}_S\mathbf{G}_W^0(0)\mathbf{V}_L[\mathbf{G}_W^0(\omega_L)&\\ +\mathbf{G}_W^0(-\omega_L)]\}|\mathbf{V}_L\rho_0\rangle\rangle)_{i,f}. \end{aligned} \tag{14}$$

The first term in the curly bracket above is the Rayleigh scattering line, centered on the frequency of the incident radiation ω_L. The second term describes the redistributed radiation and, as will be seen, has a sensitive dependence on the SDT mixing rate described by the matrix $\mathbf{W}$. For this reason, the spectral shape of the redistribution is affected more significantly by the mixing action of the microfield fluctuation, the ion dynamics, than is the absorption or emission linear-response spectral line shape [18,20]. This ion dynamics effect has not been definitively observed at the present time, although there are numerous examples of its suspected presence [23] in spectral data. In addition, the validity of the hypothesis that the Markov mixing process in the FFM accurately simulates the microfield fluctuations can be carefully examined with redistribution experiments. Another assumption, which can be validated, is that of the neglect of inelastic collisions in the impact theory operator describing the electron collisions. These inelastic collision rates mix the SDT, and would also appear in the propagators as off-diagonal elements [24], as do the elements of the transition-rate matrix. Inelastic electron collisions that couple different states of the levels belonging to the radiative transition cause the incident pump radiation to be redistributed to the various inhomogeneous components of the line even by a small inelastic collision rate and change the shape of the redistribution function. These collisions can also couple the radiative transition to states belonging to levels of other transition arrays. This coupling will then diminish the intensity of the considered transition and add to that of the coupled transition. These collisions, therefore, unlike the ion dynamics mixing, act to depopulate a particular set of levels for which the fluorescence is calculated and thereby result in an unnormalized redistribution function for that transition [25]. Thus although, in general, the argument that inelastic collision rates can be neglected because they are small compared to elastic collision rates can be valid when considering the one-photon spectrum, it may not be a good approximation for the fluorescence. The shape of the redistribution function is, therefore, a measure of the importance of inelastic collisions in addition to that of ion dynamics. Finally, it is to be

emphasized that the transition matrix **W** simulates the mixing effect of the ion microfield fluctuations on the SDT levels and transitions and is unrelated to the inelastic electron collisions. For this reason, **W** does not affect the normalization of the redistribution function.

V. REDISTRIBUTION EXAMPLES

Simple three- and four-level radiative systems are considered first in this section to illustrate the relevant quantities required for the discussion of radiation redistribution. At the end, a physical case will be also considered. To describe the photopumped fluorescence, we make use of $R(\omega_L,\omega_S)$, the redistribution function, defined by normalizing $I(\omega_L,\omega_S)$ of Eq. (14), the distribution of scattered intensity for a system perturbed by monochromatic radiation at frequency ω_L. The redistribution function,

$$R(\omega_L,\omega_S)=\frac{I(\omega_L,\omega_S)}{\int\int I(\omega_L,\omega_S)d\omega_L d\omega_S}, \tag{15}$$

is thus the joint probability density for the absorption of a photon of frequency ω_L and the emission of a photon of frequency ω_S.

For isolated lines, the redistribution function has been extensively studied and is quite well understood including for homogeneously broadened lines [25]. A fundamentally different and more complicated problem arises in the situation where several radiative transitions must be considered simultaneously. This can occur, for example, when two or more lines share the same upper level, or whenever two or more radiative transitions are coupled by a collision process with a rate high enough to perturb the radiation scattering. In both these situations, radiation absorbed by one transition can be emitted by the other and the radiative transitions cannot be considered as isolated.

To treat the general case, we define a conditional function, $P(\omega_L,\omega_S)$, in analogy with the customary factorization of the redistribution function [25],

$$R(\omega_L,\omega_S)=\phi(\omega_L)P(\omega_L,\omega_S), \tag{16}$$

where $\phi(\omega_L)$ is the normalized absorption line shape, or the probability distribution function for absorbing a photon of frequency ω_L.

For isolated lines, the conditional function is normalized, independent of the pump frequency ω_L and can be identified with $\Psi(\omega_S)$, the emission spectral function. We thus have for isolated lines, $P(\omega_L,\omega_S)=\psi(\omega_S)$. The emission spectral function is also the conditional probability distribution for observing a photon scattered at ω_S if a photon is absorbed at ω_L. This also implies that, in this case, the normalized absorption spectral distribution function $\phi(\omega_L)=\int R(\omega_L,\omega_S)d\omega_S$. In the complete redistribution limit the emission function becomes identical to the absorption function, so that the additional relation $\psi(\omega_S)=\phi(\omega_S)$ holds. The redistribution function for complete redistribution can be written, therefore, as a product of normalized absorption line-shape functions, $R(\omega_L,\omega_S)=\phi(\omega_L)\phi(\omega_S)$.

In the general case involving coupled transitions, $P(\omega_L,\omega_S)$ is not independent of ω_L, is not normalized, and cannot be interpreted as the conditional probability density.

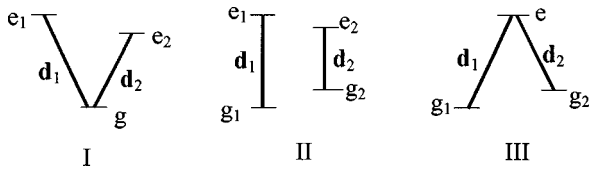

FIG. 1. Model two transition systems. The spontaneous emission rate Γ_S, Lorentzian widths γ, and resonant frequencies ω_i, are such that the two transitions are not isolated; $\delta=(\omega_1-\omega_2)/2=\omega_1/200=5\gamma=500\Gamma_S$. A 2:1 intensity ratio is chosen with $\mathbf{d}_1=\sqrt{2}\mathbf{d}_2$.

We treat this case by defining $\Pi(\omega_L,\omega_L)$, as the normalized conditional probability distribution function for the scattering of a photon at ω_S if a photon is absorbed at ω_L,

$$\Pi(\omega_L,\omega_S)=\frac{P(\omega_L,\omega_S)}{g(\omega_L)}, \tag{17}$$

where $g(\omega_L)$, is the normalization factor for the conditional function,

$$\int P(\omega_L,\omega_S)d\omega_S=g(\omega_L). \tag{18}$$

We now also have

$$\int R(\omega_L,\omega_S)d\omega_S=\phi(\omega_L)g(\omega_L) \tag{19}$$

and, since the redistribution function is always normalized,

$$\int \phi(\omega_L)g(\omega_L)d\omega_L=1. \tag{20}$$

The presence of $g(\omega_L)$ in Eq. (19) is a direct consequence of the incomplete redistribution associated with the inhomogeneous spectral structure involved in the scattering. If a process mixes the radiative transitions of the resonant pattern, then for mixing rates greater than the spontaneous emission rate $g(\omega_L)\to 1$ and $P(\omega_L,\omega_S)\to\Psi(\omega_S)=\phi(\omega_S)$, so that the redistributed fluorescence exhibits complete redistribution.

The redistribution function for a group of transitions coupled by a mixing process can be illustrated by considering the two transition systems shown in Fig. 1. The indices e and g denote, respectively, the excited and ground level, and $\mathbf{d}_1$ and $\mathbf{d}_2$ stand for arbitrarily chosen dipole moment matrix elements for the transitions with resonant frequencies ω_1 and ω_2. For the sake of simplicity, it is supposed that the two transitions have Lorentzian profiles with identical homogeneous widths γ related to the electron collision relaxation rate and a 2:1 intensity ratio, so that, $\mathbf{d}_1=\sqrt{2}\mathbf{d}_2$. The mean frequency separation of the two transitions, $\delta=(\omega_1-\omega_2)/2$, is assumed to be $\omega_1/200$. To insure that the transitions are overlapping, the mean frequency separation is taken to be of the same order as γ, the homogeneous width. Also, to make the intensity of the Rayleigh peak negligible, the spontaneous emission rate Γ_S is arbitrarily taken to be much smaller than γ. Thus, in the following example, we take $\delta=\omega_1/200=5\gamma=500\Gamma_S$. Since the description of the redistribution process has been limited to second-order, saturation

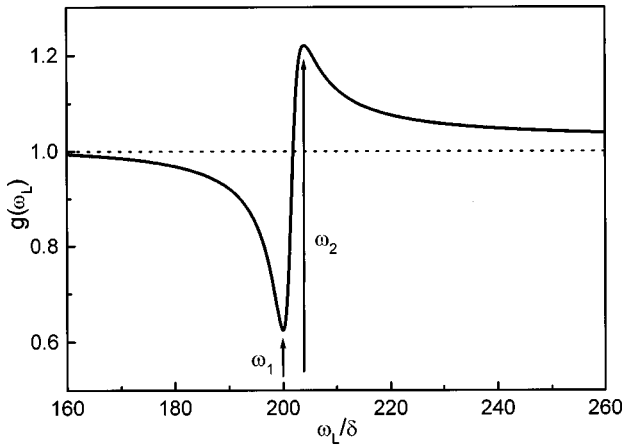

FIG. 2. Plot of $g(\omega_L)$, the normalization function for the conditional probability distribution in arbitrary units for the systems of Fig. 1 (I and II). A dimensionless laser pump frequency ω_L/δ has been used and the values of the resonance frequencies $\omega_1/\delta, \omega_2/\delta$ are indicated.

effects are not included in Eq. (14). Therefore, under this assumption, the level configurations of Fig. 1 (I and II) are equivalent. A Markovian stochastic mixing process with a unique fluctuation rate ν is applied to this configuration in order to illustrate the effect of line component mixing on the redistribution spectrum. First, however, we note that even in the limit of a negligibly weak exchange process (mixing rate much smaller than the spontaneous emission rate), the conditional function, $P(\omega_L, \omega_S)$, remains dependent on the pump frequency ω_L and the redistribution is not complete. The dependence on ω_L can be seen in Fig. 2 where the normalization function $g(\omega_L)$ is plotted against ω_L/δ for the configurations on Fig. 1 (I and II). Note that for large detunings from the resonant frequencies ω_1, ω_2, the function tends toward unity and the redistribution becomes complete. The $\nu=0$ curve of Fig. 3(b) illustrates the behavior of the conditional probability density as a function of ω_S/δ with the pump frequency fixed at one of the resonances for this case. This will be discussed in more detail in the following. Finally, the fluorescence in the model, Fig. 1 (III), with lines that share the same upper level, always displays complete redistribution. In this situation the pumping photon is scattered with the same frequency distribution as the one-photon absorption function, independent of the pump frequency, so that we have $g(\omega_L)=1$. This case can be easily modeled by equalizing the level populations in the upper manifolds of Eq. (14).

To illustrate the sensitivity of the spectral functions to the component mixing associated with the Markovian stochastic process, the configuration of Fig. 1 (II) with the previous values, $\delta=\omega_1/200=5\gamma=500\Gamma_S$, is studied as a function of the fluctuation rate parameter ν. The behavior with ν of the one-photon absorption function $\phi(\omega_L)$ and the two-photon conditional probability distribution function, $\Pi(\omega_S, \omega_L)$, is depicted in Figs. 3(a) and 3(b), respectively. The spectrum of the absorption function starts out at small ν with the two Stark components present in the defined intensity ratio, 2:1. With increasing ν, the coupling associated with the fluctuation process causes the two components to broaden and coalesce. The effect of component mixing becomes important

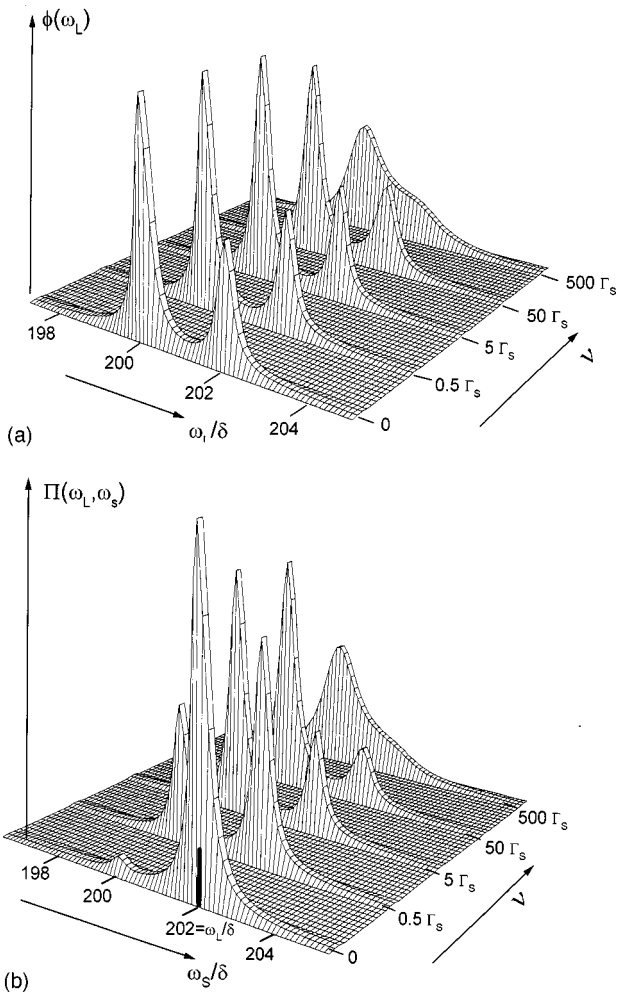

FIG. 3. (a) For the model system in Fig. 1 (II), the one-photon profile function $\phi(\omega_L)$ is plotted against the dimensionless laser pump frequency ω_L/δ in units of the inverse mean frequency separation δ^{-1} for five mixing rates of the two components. (b) For the model system in Fig. 1 (II), the two-photon conditional probability distribution function, $\Pi(\omega_L, \omega_S)$, is plotted in units of the inverse mean frequency separation δ^{-1} against the dimensionless frequency ω_S/δ for a fixed pump frequency at $\omega_L=\omega_2$, with the same range of fluctuation rates as in Fig. 3(a).

when that is when the fluctuation rate is of the same order of magnitude as the component separation. At this value of ν (equal to δ, or $500\Gamma_S$), the two components have completely merged. The behavior is different for the two-photon redistributed fluorescence spectrum presented in Fig. 3(b) which has been calculated for the pump frequency resonant with ω_2. Here it can be seen that for a null or vanishingly small fluctuation rate, the fluorescence profile consists almost entirely of the pumped spectral component and has only a small contribution from the other component, arising from the overlapping of the homogeneous widths. Thus, with a small fluctuation rate the fluorescence spectrum differs drastically from the absorption profile with the same ν, indicating that the redistribution is incomplete. Increasing the mixing rate causes the unpumped Stark component to grow in intensity relative to the pumped component until at large ν, the fluorescence and absorption spectral profiles become indistinguishable and the redistribution becomes complete. It can be seen in Fig. 3(b) that the fluorescence spectrum becomes

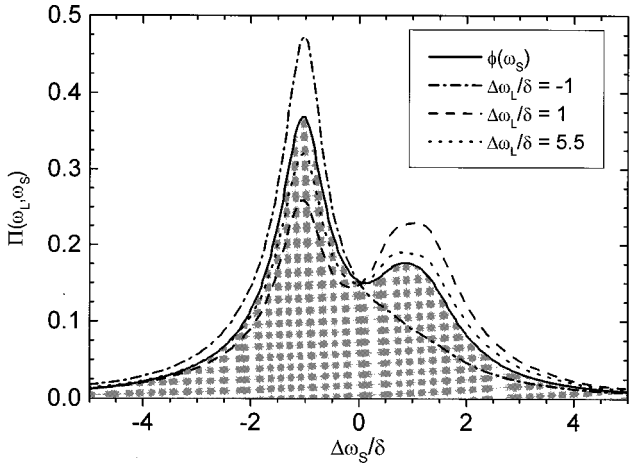

FIG. 4. Absorption profile $\phi(\omega_L)$ and conditional probability distribution function $\Pi(\omega_L,\omega_S)$ for the $3d$-$2p$ Balmer α transition of CIV in a plasma with parameters, $N_e=5.10^{19}\,\mathrm{cm}^{-3}$ and $T_e=10$ eV. The distributions are plotted as a function of $\Delta\omega_S/\delta$, the dimensionless detuning of the fluorescence frequency from the line center of gravity, $\omega_0=(\omega_2+\omega_1)/2$. The absorption profile, in units of δ^{-1}, is indicated by the solid filled curve, and the conditional probability, $\Pi(\omega_L,\omega_S)$, in the same units, is presented for three pump frequency detunings from the line center of gravity, $\Delta\omega_L=-\delta$, δ, and 5.5δ. The atomic physics parameters for this Balmer α transition are $\omega_1=1033.7\times10^{14}$ rad/s (182.22 Å) and $\omega_2=1034.5\times10^{14}$ rad/s (182.09 Å), so that $\omega_0=(\omega_2+\omega_1)/2=1034.1\times10^{14}$ rad/s and $\delta=(\omega_2-\omega_1)/2=0.4\times10^{14}$ rad/s.

identical to the absorption line profile when the fluctuation rate is greater than the lifetime of the upper level ($\nu>50\Gamma_s$).

The above examples are useful to clarify the principal intuitive concepts, and to illustrate the contribution of the various line-broadening mechanisms to the redistribution, e.g., the homogeneous broadening of the inhomogeneous spectral components and the mixing of these components by a dynamic effect. The next example will illustrate the use of the redistribution model for the investigation of a more realistic physical case, the $3d$-$2p$ Balmer alpha transition of hydrogenlike carbon. This has been previously discussed in connection with gain studies associated with the development of an x-ray laser [26]. Because this transition does not involve the ground state, it is more appropriate for studies related to radiation transfer than for a frequency redistributed single scattering measurement where the signal intensity would likely be small. We investigate this case here because of its simplicity and to illustrate some of the more important elements relevant to radiation redistribution. For the study we assume a plasma with parameters such that the electron density $N_e=5\times10^{19}\,\mathrm{cm}^{-3}$ and the electron temperature $T_e=10$ eV. For these plasma conditions, ion dynamics is negligibly small, and the spectral inhomogeneity of the radiative pattern is associated with the Stark-broadened fine structure. In Fig. 4, the calculated normalized absorption line shape (the absorption probability distribution) for this transition is presented as the gray-filled profile. The absorption spectrum consists of two resonances that are the result of the ion Stark effect broadening and the merging of two distinct electron-broadened fine-structure components.

The redistribution dependence on the pump frequency is

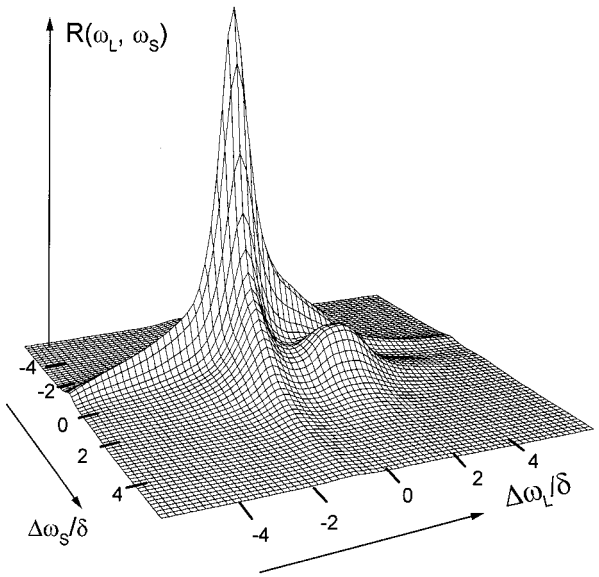

FIG. 5. Three-dimensional plot of the redistribution function, $R(\omega_L,\omega_S)$, for the Balmer α transition of Fig. 4 with the same plasma conditions. Dimensionless pump and probe frequencies are used on the x and y axes, and the redistribution function is plotted in units of δ^{-2}.

also given in Fig. 4 where the normalized two-photon conditional probability density, $\Pi(\omega_L,\omega_S)$, is calculated for three different pump frequencies ω_L. The absorption function $\phi(\omega_S)$ is plotted on the same graph for comparison. Two of the pump frequencies are chosen to coincide with the unshifted frequencies of the fine-structure components at 182.22 and 182.09 Å ($\Delta\omega_L/\delta=1$ and -1). The third pump frequency is chosen to have a detuning of -0.31 Å ($\Delta\omega_L/\delta=5.5$) from the ω_2 resonance. It is clear from a comparison of the absorption profile with the conditional probability density in Fig. 5 that the redistribution is partial for pumping near the resonances. This is to be expected because ion dynamics is absent for the plasma conditions chosen so that no mechanism exists to transfer of population between the two resonances. The conditional probability distribution tends toward the absorption probability density profile (complete redistribution) as the detuning from the resonances becomes large since then both resonances are pumped almost equally. Finally, the two-dimensional redistribution function, $R(\omega_L,\omega_S)$, is given in Fig. 5. This surface represents the frequency-dependent resonance radiation redistribution function for the CIV Balmer α transition in the same hot, dense plasma conditions used in Fig. 4. This function is the required input for calculations of radiation transfer.

VI. DISCUSSION

The FFM approach, which has been used successfully in the past to provide complex ionic absorption or emission spectral line shapes for emitters in hot, dense plasmas, has been extended here to enable calculations of radiative redistribution. The system of dressed two-level emitters or SDT defined in the FFM includes the partial inhomogeneities of the line-broadening process, and constitutes the most important simplification permitting a straightforward extension to different plasma conditions, laser pump frequencies, and

ionic emitters. Relatively uncomplicated calculations of the photopumping of complex multielectron ionic systems can be performed with the method presented. Saturation effects for large Rabi frequencies such as those related to the ac Stark effect splitting of lines were excluded, but could easily be handled within the framework of the present calculations. The computational method developed constitutes a powerful tool for the investigation of radiative transport in plasmas. In particular, for the study of the ion dynamics effect, redistribution provides a more sensitive probe than the one-photon spectra of the FFM. In particular, the study of the effect of the fluctuating microfields or ion dynamics on the redistribution of incident resonance radiation requires plasma conditions for which the line transitions have substantial ion Stark broadening. This often dominates the one-photon spectral line profile, obscuring the perturbative effects of the microfield fluctuations. However, the spectral content of the redistribution function for the same transition has been shown to be more sensitive to the ion dynamics effect. Related to this are possible investigations that would permit radiative transfer to be studied for plasma conditions where a sufficiently slow mixing of inhomogeneous spectral-line components results in partial redistribution.

As an application of the theory, the feasibility of a photopumping experiment, targeting a resonance between the $3d$-$2p$ line of Mg IV (146.526 Å) and a Zr x-ray laser line at 146.515 Å, was calculated and has been published elsewhere [10]. The plasma conditions used in that calculation were limited to the study of only ground-state transitions of a weakly ionized emitter and also by the available x-ray laser wavelengths. For these plasma parameters, ion Stark broadening is a small contribution to the line profile and, therefore, ion dynamics is negligible. Nevertheless, an experimental study of the redistribution function was shown to be feasible. The pumping efficiency and fluorescence yield are such that even with a high-resolution spectrometer, the fluorescence photons would be observable. The Mg IV line is composed of a number of overlapping fine-structure transitions and Stark components, yielding a resonance fluorescence spectrum that is sensitive to the photopumping of particular inhomogeneous components. This is more evident at lower plasma electron density where the homogeneous broadening does not merge the fine structure into a single resonance, but also at higher-electron density, a subtle difference from complete redistribution attributable to the inhomogeneous nature of the transition has been shown to exist.

Experiments such as that discussed in Ref. [10], where partial redistribution is predicted because of the fine-structure inhomogeneity, are of experimental interest due to the possibility of testing the basic assumptions in traditional line-shape theories. One example is the assumption that inelastic collisions can be ignored, which results in the prediction that there can be no fluorescence from unpumped states. Thus, in plasmas with kinetics are such that inelastic collisions are significant; this would manifest itself as an additional fluorescence component from these states. The intensity of these additional components would be a measure of the contribution of the inelastic collisions to the redistribution process. A second example of what a critical test redistribution experiment could provide is found in the standard Stark-broadening theory assumption that the ions are static and the electrons impact. This hypothesis results in a spectrum with distinct Stark components that merge under common plasma conditions. At present, no observation of the merged individual components, which compose the spectral line profile, has been possible. A redistribution experiment could result in a measurement of these inhomogeneous components and would be a simple confirmation of this basic theoretical line-broadening concept. Cases, which could have observable redistribution spectra with interesting plasma conditions, are under active investigation at present. There is a narrow range of plasma conditions, however, that give rise to partial redistribution due to an ion Stark effect, so that an experimental observation of this effect will remain a difficult problem.

ACKNOWLEDGMENTS

Part of this work was performed under the auspices of the U.S. Department of Energy at Lawrence Livermore National Laboratory under Contract No. W-7405-Eng-48. L. Klein was supported in part by the U.S. Department of Energy under the Inertial Fusion Science Supporting Stockpile Stewardship Grant Program, and by the LLNL Research Collaboration Program for HBCU's.

[1] B. Talin, A. Calisti, L. Godbert, R. Stamm, R. W. Lee, and L. Klein, Phys. Rev. A **51**, 1918 (1995).
[2] A. Calisti, L. Godbert, R. Stamm, and B. Talin, J. Quant. Spectrosc. Radiat. Transf. **51**, 59 (1994).
[3] L. Godbert, A. Calisti, R. Stamm, B. Talin, R. Lee, and L. Klein, Phys. Rev. E **49**, 5644 (1994).
[4] L. Godbert, A. Calisti, R. Stamm, B. Talin, J. Nash, R. Lee, L. Klein, S. Glenzer, and H.-J. Kunze, Phys. Rev. E **49**, 5889 (1994).
[5] S. Glenzer, Th. Wrubel, S. Büscher, H.-J. Kunze, I. Godbert, A. Calisiti, R. Stamm, B. Talin, J. Nash, R. Lee, and L. Klein, J. Phys. B **27**, 5507 (1994).
[6] C. Back, R. Lee, and C. Chenais-Popovics, Phys. Rev. Lett. **63**, 1471 (1989); C. Back, C. Chenais-Popovics, and R. Lee, Phys. Rev. A **44**, 6730 (1991); C. Back, J. Castor, P. Dykema, R. Klein, and R. Lee, *ibid.* **44**, 6743 (1991).
[7] R. Elton, *X-Ray Lasers* (Academic, San Diego, 1990).
[8] J. Koch, R. Lee, J. Nilsen, J. Moreno, B. MacGowan, and L. Da Silva, Appl. Phys. B: Lasers Opt. **B58**, 7 (1994).
[9] R. Kelly, J. Phys. Chem. Ref. Data Suppl. **16**, 1 (1987).
[10] C. Mossé, A. Calisti, M. Koubiti, R. Stamm, B. Talin, J. Koch, R. Lee, and L. Klein, J. Quant. Spectrosc. Radiat. Transf. **58**, 803 (1997).
[11] D. Benredjem *et al.*, J. Phys. B **29**, 4587 (1996); D. Benredjem *et al.*, J. Quant. Spectrosc. Radiat. Transf. **55**, 439 (1996).
[12] R. Stamm, B. Talin, E. Pollack, and C. Iglesias, Phys. Rev. A **34**, 4144 (1986).
[13] A. Calisti, F. Khelfaoui, R. Stamm, and B. Talin, in *Spectral Line Shapes*, edited by L. Frommhold (AIP, New York, 1990), Vol. 6, pp. 3–18.

[14] L. Carlsten, A. Szöke, and M. G. Raymer, Phys. Rev. A **15**, 1029 (1977).
[15] M. Osterhold, G. Himmel, and H. Schlüter, J. Quant. Spectrosc. Radiat. Transf. **41**, 425 (1989).
[16] M. Ruffert, G. Himmel, M. Osterhold, and H. Schlüter, J. Quant. Spectrosc. Radiat. Transf. **42**, 327 (1989).
[17] R. W. Lee and E. Oks, Phys. Rev. E **58**, 2441 (1998).
[18] B. Talin and L. Klein, Phys. Rev. A **26**, 2717 (1982).
[19] I. Hubeny, in *Spectral Line Shapes*, edited by F. Rostas (Walter de Gruyter & Co., Berlin, 1985), Vol. 3, pp. 501–522.
[20] B. Talin, Y. Botzanowsky, C. Calmes, and L. Klein, J. Phys. B **16**, 2313 (1983).
[21] B. Talin, R. Stamm, V. Kaftandjian, and L. Klein, Astrophys. J. **322**, 804 (1987).
[22] A. Ben-Reuven, Phys. Rev. A **22**, 2585 (1980).
[23] N. C. Woolsey, B. A. Hammel, C. J. Keane, A. Asfaw, C. A. Back, J. C. Moreno, J. K. Nash, A. Calisti, C. Mossé, R. Stamm, B. Talin, L. Klein, and R. W. Lee, Phys. Rev. E **56**, 2314 (1997).
[24] S. Alexiou, Phys. Rev. A **49**, 106 (1995).
[25] A. Omont, E. Smith, and J. Cooper, Astrophys. J. **175**, 185 (1972).
[26] D. H. Oza, R. L. Greene, and D. E. Kelleher, Phys. Rev. A **34**, 4519 (1986).